Synthesis and Design of a Synthetic-Living Material Composed of Chitosan, *Calendula officinalis* Hydroalcoholic Extract, and Yeast with Applications as a Biocatalyst

Isabel O. Caamal-Herrera, Mariana B. Erreguin-Isaguirre, Angel León-Buitimea, and José R. Morones-Ramírez*

ACCESS | Metrics & More | Article Recommendations

ABSTRACT: Design and development of materials that couple synthetic and living components allow taking advantage of the complexity of biological systems within a controlled environment. However, their design and fabrication represent a challenge for material scientists since it is necessary to synthesize synthetic materials with highly specialized biocompatible and physicochemical properties. The design of synthetic-living materials (vita materials) requires materials capable of hosting cell ingrowth and maintaining cell viability for extended periods. Vita materials offer various advantages, from simplifying product purification steps to controlling cell metabolic activity and improving the resistance of biological systems to external stress factors, translating into reducing bioprocess costs and diversifying their industrial applications. Here, chitosan sponges, functionalized with *Calendula officinalis* hydroalcoholic extract, were synthesized using the freeze-drying method; they showed small pore sizes (7.58 μm), high porosity (97.95%), high water absorption (1695%), and thermal stability, which allows the material to withstand sterilization conditions. The sponges allowed integration of 58.34% of viable *Saccharomyces cerevisiae* cells, and the cell viability was conserved 12 h post-process (57.14%) under storage conditions [refrigerating temperature (4 °C) and without a nutrient supply]. In addition, the synthesized vita materials conserved their biocatalytic activity after 7 days of the integration process, which was evaluated through glucose consumption and ethanol production. The results in this paper describe the synthesis of complex vita materials and demonstrate that biochemically modified chitosan sponges can be used as a platform material to host living and metabolically active yeast with diverse applications as biocatalysts.

1. INTRODUCTION

The synergy and overlap between the technologies developed in the chemical and materials sciences have led to the understanding and development of new advanced materials.[1] The challenge in developing novel and dynamic materials is continuously improving their properties and efficiency and broadening their applications. One approach to achieve this is to couple synthetic materials with complex systems, such as biological systems. Coupling synthetic and biological systems is one of the most relevant and exciting challenges in developing the next generation of materials.[1−3] Market conditions and technological progress demand the use of increasingly complex

and dynamic materials that are reusable, productive, and produced sustainably.[1,4,5]

The use of integrated cells into materials to construct synthetic-living systems has broad applications in biotechnological and industrial processes such as fermentation, water

treatment, bioremediation, and delivery systems. Moreover, integrating living systems and synthetic materials is crucial in improving processes and developing practical tools to decrease operating costs.[6−9] This integration brings together advantages in critical areas such as purifying steps, developing continuous or semicontinuous conditions, incrementing material reusability, enhancing the metabolic activity of microorganisms, and augmenting their resistance to external stress and process variables.[7,8]

Numerous chemical and physical techniques for integrating living cells have been developed within the last decades. The entrapment of microorganisms and cells in calcium alginate beads is the most used technique due to its simplicity; nevertheless, it presents several disadvantages, such as complications with nutrient diffusion and non-optimal bio-compatibility.[10] The adsorption (physical or covalent binding) of the microbial cells on supports (as films and membranes) is a technique also used frequently with this goal. Nevertheless, factors such as support properties, microbial cell surface, and environmental conditions affect the efficiency of the process.[11,12]

Concerning the support materials, the critical factors for cell integration include their porosity and capacity to adhere to cells through van der Waals interactions, ionic forces, hydrogen bonding, or other mechanisms.[12,13] The porous matrices have a high permeability that allows diffusion of oxygen and nutrients needed characteristics when into the material are encapsulated microorganisms for water purification, biomolecule production, and ethanol production.[14] Other applications of these matrices are in tissue engineering, drug delivery systems, wound healing, as well as in the production of probiotic food, biosorption and bioremediation of chemicals, and antimicrobial food packaging.[14] The most common techniques for the fabrication of porous materials are solvent casting, particulate leaching, gas foaming, phase separation, electrospinning, porogen leaching, fiber mesh, rapid prototyping, and freeze drying, which are adequate to the requirements of different applications.[15]

A polymer used in the elaboration of porous, reliable, and safe materials is chitosan, which is derived from chitin (a natural biopolymer) using a deacetylation process. Between principal characteristics are non-toxic, biodegradable, versatile, and biocompatible.[16,17] Its cationic nature and the presence of amino groups impart interesting properties to form structures such as films, hydrogels, nanoparticles, microbeads, sponges, and membranes, which can be used to incorporate microbial cells by techniques of entrapment and adsorption.[18,19] However, some authors have reported low cell adhesion capacities, which have been addressed by mixing it with other non-degradable and biodegradable polymers, as well as other compounds.[20−22]

In recent years, plant extracts have been used to modify the physicochemical properties of materials, enhancing their ability to integrate cells by increasing cell adhesion and cell viability within the material.[23,24] Calendula officinalis (C. officinalis) is an important medicinal plant with potential biological properties; its hydroalcoholic extract has been used to elaborate films with improved adhesion and viability for human fibroblasts as well as other eukaryotic cells such as Candida albicans.[23] Aloe vera was another plant used in the preparation of chitosan films, in this case, to maintain the viability and antifungal activity of Lactobacillus paracasei TEP6, a microorganism integrating into the material; this biomaterial has been used as a coating for vegetables to prevent the growth of the Colletotrichum gloeosporioides fungi.[24]

Microbial biosynthesis uses different microorganisms to produce a large variety of industrial products for human interest.[25] Saccharomyces cerevisiae (S. cerevisiae) is a non-pathogenic yeast and the best-studied eukaryote. It is the most valuable species for several biotechnological purposes and industrial applications.[26,27] S. cerevisiae has been integrated into cross-linked materials based on chitosan obtained through chemical methods; however, these methods use compounds that subsequently do not allow scaling up the use of the materials for their applications in the food or pharmaceutical industries.[28,29] Therefore, the material, integration conditions, and characterization of the integrated cells should be optimized to improve the metabolic functions of the cells as well as the industrial process conditions.

In the present work, we functionalized chitosan sponges with the hydroalcoholic extract of C. officinalis (HAECa) flowers to modify their physicochemical properties. As a result, the designed sponges displayed integration and preservation of S. cerevisiae cell viability for prolonged times under limiting storage conditions (nutrients and temperature). In addition, the composed material had biocatalytic applications since it was able to consume glucose and produce ethanol even 7 days after the integration process. Our synthetic-living system (vita material) incorporates a functionalizing agent of natural origin; therefore, the designed and synthesized vita material has the potential to be used for applications as a biocatalyst in various types of industries, including food processing and packaging as well as the pharmaceutical sector.

2. RESULTS AND DISCUSSION

2.1. Synthesis and Macroscopic Characteristics of HAECa-Functionalized Chitosan Sponges.
Using the freeze-drying method, we synthesized chitosan sponges, both non-functionalized and functionalized with the hydroalcoholic extract of C. officinalis (HAECa) (Figure 1). The chitosan
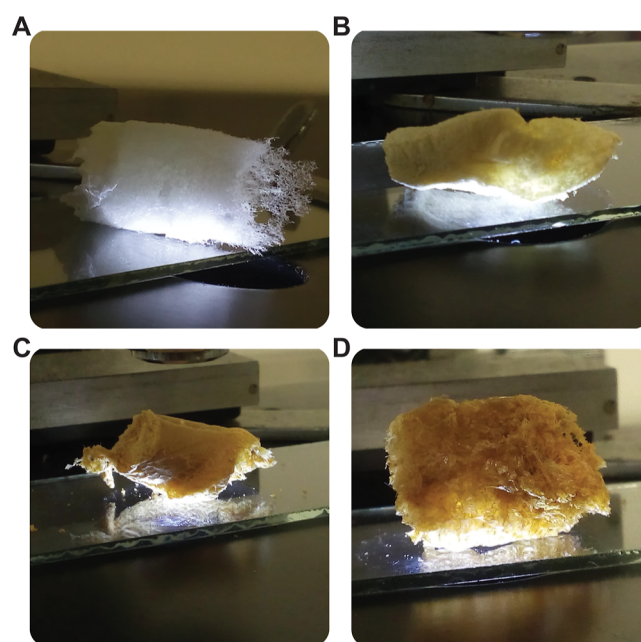
Figure 1. Macroscopic characteristics of chitosan sponges prepared by the freeze-drying method. (A) Chitosan control, (B−D) chitosan sponges synthesized with various concentrations (v/v %) of C. officinalis extract (HAECa).

sponge control (Figure 1A) and the HAECa-functionalized chitosan sponges prepared with 8% v/v (Figure 1B), 10% v/v (Figure 1C), and 12% (Figure 1D) displayed differences in their macroscopic characteristics, including color, shape, and porous structure. The HAECa-functionalized chitosan sponges have a yellow-brown tone and stretchy form compared to the chitosan sponge control (light-colored and porous). In addition, an increase in color intensity and elastic form is observed and correlates with increments in extract concentration (%v/v).

The HAECa-functionalized chitosan sponge color can be attributed to the chemical composition of the extract. Some authors have reported the presence of lutein, a xanthophyll present in the ethanolic extract, which has an orange−red color that absorbs blue light, developing a yellow color at low concentrations and an orange−red at high concentrations.[30] The shape of these sponges can be attributed to a plasticizer effect of the extract concentration. Commonly, plasticizers such as water and polyols (glycerol and sorbitol) contain OH groups within their chemical structures, which can affect the continuity of the polymer matrix leading to physical changes, such as materials becoming more flexible and stretchable.[31]

Density, a macroscopic property, was evaluated in both the control and the functionalized chitosan sponges. This property was calculated from the mass-to-volume ratio of the sponge samples. The control presented a value of 0.14 ± 0.03 g cm^{-3}, which was similar in the sponges functionalized with 8 and 12% HAECa (Figure 2), while the density of the sponges
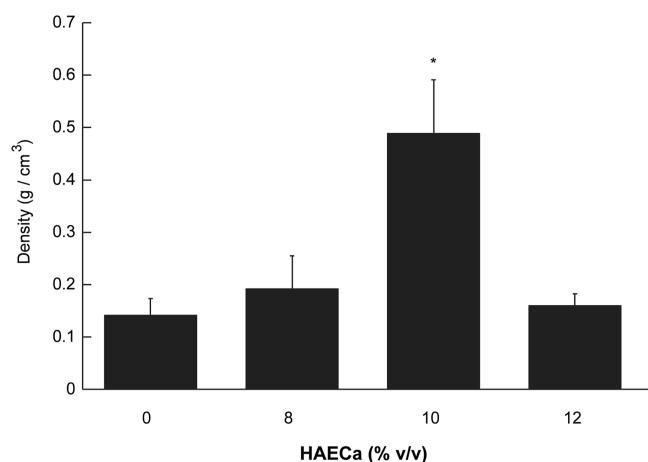
Figure 2. Density of chitosan sponges prepared by the freeze-drying method. * indicates significant difference from control and rest of the HAECa concentrations tested.

functionalized with 10% of the extract (0.49 ± 0.10) was significantly different from the control and the rest of the functionalized sponges. An increase in sponge density may contribute to the improvement of mechanical properties such as dimensional stability.

2.2. Microstructure and Elemental Composition of HAECa-Functionalized Chitosan Sponges. The microstructure of the chitosan sponges was studied by scanning electron microscopy (SEM), and their elemental composition was determined by energy-dispersive spectroscopy (EDS). The chitosan sponges presented a heterogeneous porous structure (Figure 3) with an average pore diameter of 21.98 ± 2.16 μm for the chitosan sponge control (Figure 3A). Moreover, the HAECa-functionalized sponges showed an average pore size of 7.58 ± 1.56 μm (Figure 3C) at 8% (v/v) HAECa

concentration and a 40.52 ± 7.41 μm (Figure 3E) and 29.67 ± 5.14 μm (Figure 3G) average pore sizes at 10% v/v and 12% v/v concentrations, respectively. Furthermore, energy-dispersive X-ray spectrum (EDS) studies demonstrated the presence of Na, K, Mg, and Cl in the HAECa-functionalized chitosan sponges (Figure 3D,F,H), whereas these elements were not found in the control sponges. The occurrences of C and O in the 12% v/v HAECa-functionalized chitosan sponges (Figure 3H) were 49.55 and 28.01%, respectively, these values were the lowest compared to the functionalized sponges with 8 and 10% of HAECa. Concerning Cl and K, the presence was increased on HAECa functionalized sponges in concordance with the increase in concentrations of HAECa.

Pore size is an important parameter to consider in the integration phase of microorganisms or living systems into a material, such as sponges. It is desirable to have a pore size that allows oxygen and nutrient diffusion for survival, growth, and proliferation of cells within the material.[14,32,33] Some authors indicate that porosity, pore architecture, and pore interconnectivity have a significant role in the survival and proliferation of cells.[22] Concerning the biomedical application of porous materials, a small pore can aid in the differentiation (mechanism involved in the cell regeneration process) of human cells, and large pores have been shown to inhibit cell proliferation (increase in the number of cells) between cells of the same kind.[32,34] In the present study, we report pore sizes (13−24 μm) and microstructures of the chitosan sponge controls (Figure 3A) and show the differences observed from other studies that synthesize the chitosan sponges under similar processing conditions and cross-linking agents (genipine).[35] The results indicate that the following parameters: conditioning temperature before the freeze-drying process, chitosan concentration, and the addition of different substances (cross-linking agent and natural extract) modify the characteristics of the sponge, including porosity, morphology, density, and elasticity.[36−38] The pore size (6.81−9.95 μm) observed in HAECa-functionalized chitosan sponge at 8% v/v (Figure 3C) could be attributed to the hydrophilic nature of the extract. The hydroalcoholic extract contains OH groups that can associate with the chitosan (amino and carboxyl groups) and the medium (water) through hydrogen bonds; therefore, after applying low-temperature conditions (-20 °C) and further freeze-drying, the process can cause the formation of smaller pores with little or no cell walls. On the other hand, the porous size and wall structure in HAECa-functionalized chitosan sponges at 10% v/v (Figure 3E) and 12% v/v (Figure 3G) can be attributed to the plasticizing effect of the extract on the chitosan polymer chains due to an increase of the concentration and the presence of elements as Na and K (Figure 3F,H).[39,40] The plasticization allows the flexibility and aperture of the chains and, therefore, an increment in pore size.[31] Previous studies using mixtures of chitosan and other hydrophilic biopolymers have reported similar behaviors.[37,41]

The addition of the HAECa extract caused a change in the elemental composition of the chitosan matrix (Figure 3); this behavior has been observed previously in other studies which use spinach extract.[42] The appearance of minerals (Figure 3D,F,H) allows the association with the chemical composition of the HAECa.[43] The presence of Na, Mg, Cl, and K in the material could affect its water absorption capacity by interacting with carboxyl and amino groups of the chitosan through electrostatic forces. These effects reduce the interaction sites of this biopolymer with the aqueous medium. The material thermal
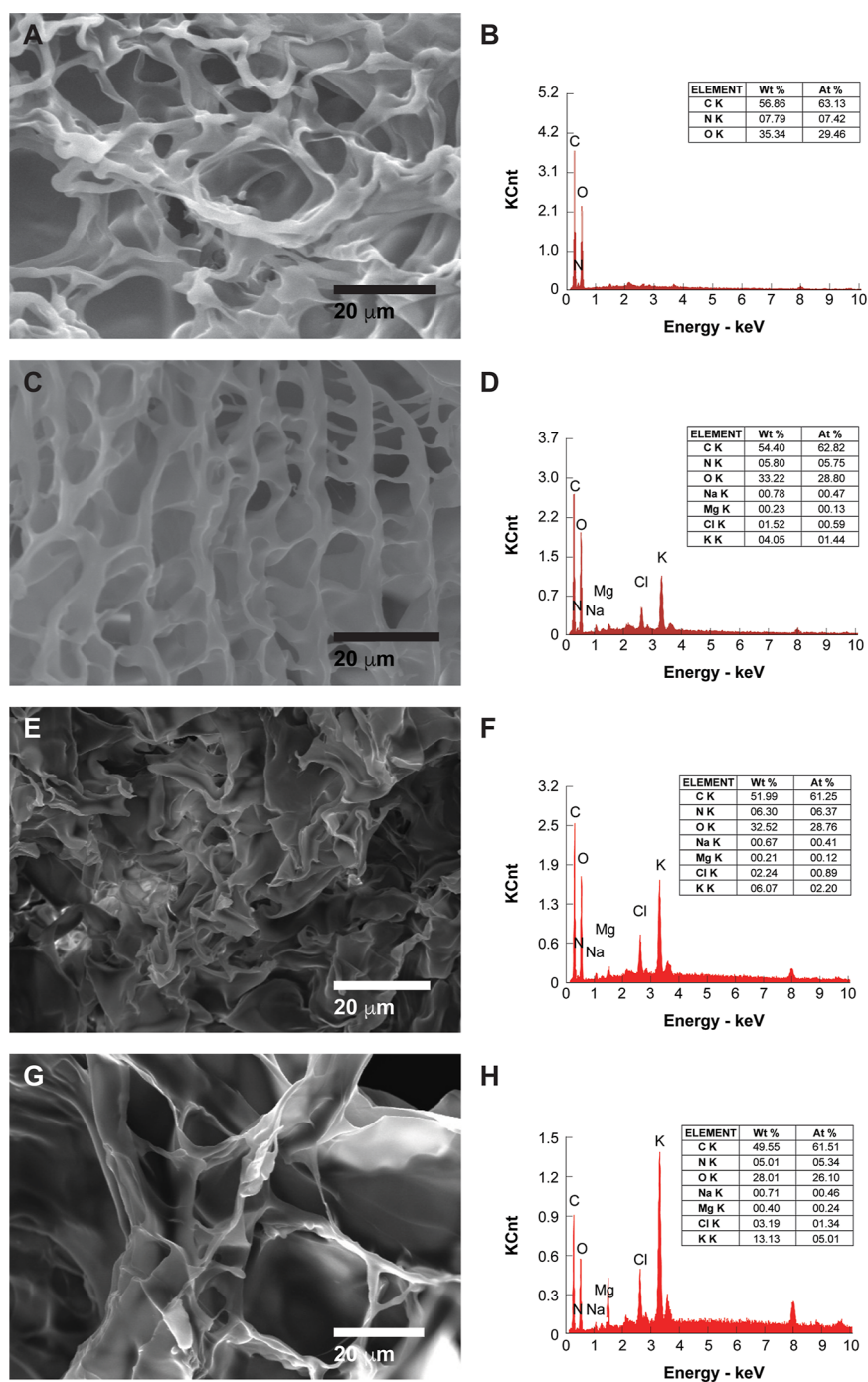
Figure 3. SEM and EDS analysis of chitosan sponges functionalized with hydroalcoholic extract of *C. officinalis* (HAECa) flowers. (A,B) Chitosan control, (C,D) 8% v/v, (E,F) 10% v/v, and (G,H) 12% v/v.

properties such as decomposition temperature and glass transition temperature could suffer changes by the plasticizing effect of these elements. The integration of the microorganisms into the material and the conservation of their cell viability could also be affected.

2.3. Chemical and Thermal Characterization of HAECa-Functionalized Chitosan Sponges. Fourier transform infrared (FTIR) spectroscopy showed the characteristic peaks corresponding to the functional groups reported in chitosan (Figure 4A).[44] The spectra display an increase in the intensity of the bands for the functionalized chitosan sponges as the concentration of the HAECa is increased. However, the

transmittance of the characteristic peaks of chitosan at 3300–3200 cm^{-1} (corresponding to N–H and O–H stretching, intramolecular hydrogen bonds), 2974–2958 cm^{-1} (linked to C–H symmetric and asymmetric stretching of chitosan), 1589–1598 cm^{-1} (from primary amide groups), 1524–1543 cm^{-1} (–NH of amide II group), 1372–1386 cm^{-1} (C–N stretching of amide III group), 1067–1079 cm^{-1} (C–O–C bond), 1028–1037 cm^{-1} (C–O), and 910–742 cm^{-1} (C–H and C=C bonds) were decreased for the HAECa-functionalized chitosan sponges. Moreover, the peaks at 3295 cm^{-1} (corresponding to the stretching of NH and OH bonds) and 1660 (linked to C=O stretching in the amide I) shifted significantly to 3302 and 1721
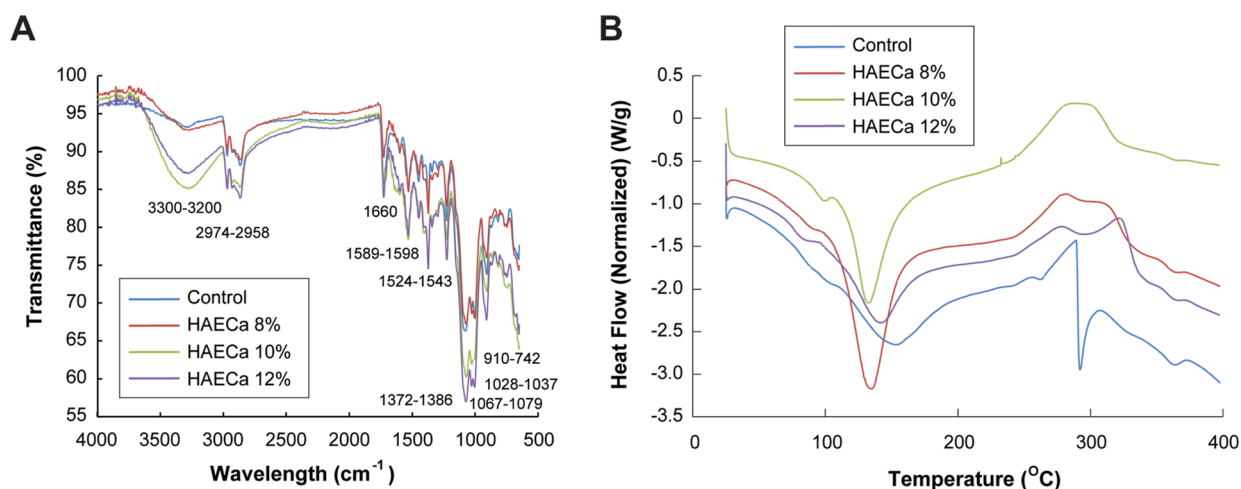
Figure 4. (A) FTIR of chitosan sponges functionalized with the hydroalcoholic extract of *C. officinalis* (HAECa) flowers, and (B) DSC analysis.
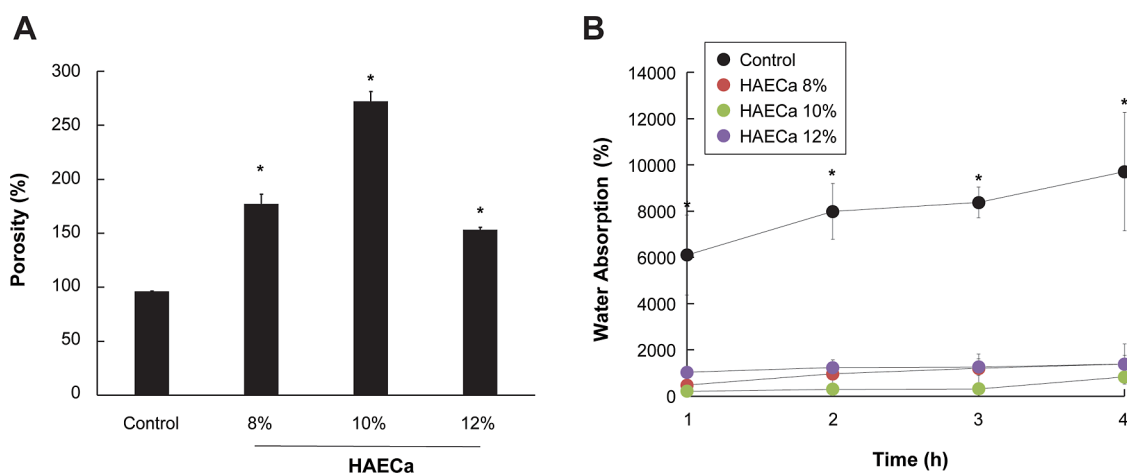
Figure 5. (A) Porosity and (B) water absorption of chitosan sponges functionalized with the hydroalcoholic extract of *C. officinalis* (HAECa) flowers.

cm^{-1}, respectively (Figure 4A). Differential scanning calorimetry (DSC) was used to characterize the sponges and report their physical-chemical responses to polymer heating.[45] The DSC thermogram of the chitosan sponge control (Figure 4B) shows two endothermic peaks at 95 and 151 °C (ΔH 196 J/g). In addition, exothermic peaks were observed at 260 °C (ΔH 4 J/g), 307 °C (ΔH 156 J/g), and 370 °C (ΔH 14 J/g). For the HAECa-functionalized chitosan sponges, the DSC thermogram shows two endothermic peaks, the first at 96−97 °C (ΔH 3−7 J/g) and the second (broader endothermic peak) at 130−140 °C (ΔH 182−336 J/g). In addition, two exothermic peaks were observed at 280−320 °C (ΔH 185−209 J/g) and 350−370 °C (ΔH 1−2 J/g).

In general, the FTIR spectrum of HAECa-functionalized chitosan sponges showed a widening of chitosan characteristic bands and a decrease in the transmittance, especially in the band at 3300−3000 cm^{-1}, when the extract concentration was increased. This could be attributed to the hydrophilic nature of the extract and its chemical composition.[30] Compounds such as saccharides, carboxylic acids, antioxidants, water, and ethanol could form hydrogen bonds with the chitosan matrix due to the presence of OH groups in their chemical structures. This behavior was observed previously in a study of chitosan-starch films with natural extracts.[46]

In DSC analysis, the first endothermic peak observed in the chitosan sponges with HAECa (96−97 °C) can be attributed to the evaporation of solvent trace in the material such as water (principally), acetic acid, and ethanol; as well as other low weight compounds (such as volatile components) of the extract.[47] The second endothermic peak (130−150 °C) is related to the glass transition temperature of the relaxation of the chitosan chains and some components from the extract present in the chitosan network.[48] The exothermic peaks observed (280−320 and 350−370 °C) can be associated with the disruption and decomposition (thermal and oxidative) of chitosan and the vaporization and elimination of volatile products generated.[49] The extract induced an increase in the first exothermic temperature and a decrease in the second endothermic temperature by a plasticizer effect on the chitosan network due to its hydroalcoholic nature and chemical composition.[50,51] Still, it conserved the thermal stability of the material, which is very important for its application in the integration of biological systems, especially when the material requires undergoing processes such as sterilization through heat treatments, which is a preparatory phase of the integration process of the biological system.[52,53]

2.4. Porosity and Water Absorption of HAECa-Functionalized Chitosan Sponges. The porosity of the chitosan sponge control using the liquid displacement method

with ethanol was 90.34% (Figure 5A). The addition of HAECa to the chitosan matrix did not show a statistically significant increase in the porosity of the sponges, compared to the control (Figure 5A). The porosities of 8, 10, and 12% v/v HAECa-functionalized chitosan sponges were 89.37, 97.95, and 88.65%, respectively. Moreover, the chitosan sponge controls exhibited high water absorption (9706%), causing the material to change its shape to a hydrogel. The addition of HAECa decreases the water absorption rate compared with the chitosan sponge control ($p < 0.05$). Water adsorption is inversely proportional to the HAECa concentration (v/v %) present in functionalized chitosan sponges, as shown in our results where chitosan sponges with 8, 10, and 12% v/v HAECa displayed water absorptions of 1388, 1388, and 827%, respectively (Figure 5B).

The porosity in a material allows better transport of nutrients and exchange of gases, metabolites, and metabolic waste between the integrated cells, which is critical for their growth and proliferation.[32,33,38] Some authors have pointed out that a greater than 80% porosity is ideal when the sponge is used as a cellular scaffold.[54,55] In this study, the addition of HAECa to the chitosan matrix did not significantly modify the porosity values of the sponges; nevertheless, the shape, size, and structure of the pores changed (Figure 3A,C,E,G). The porosity values observed in our study were higher than that of a previous study with *A. vera* and tetracycline hydrochloride (68.74 and 56.44%). In this, the extract and the antibiotic increased the porosity percentage of the sponge, which was the opposite of the behavior observed in our study.[56]

Water absorption is a crucial parameter for sponges since the culture media used for cell growth are in an aqueous medium. Therefore, materials synthesized for this purpose must show the ability to maintain structural stability in aqueous environments and allow cell growth. The higher water absorption observed in the chitosan sponge control can be explained by its un-crosslinked structure and its hydrophilic nature induced by the carboxyl and amino groups interacting with an aqueous medium. The quantity of water trapped in the sponge could cause the collapse of the material structure, which was observed in the present study (with chitosan control sponge) and previously in studies using other hydrophilic biopolymers.[32] The addition of HAECa extract induced a decrease in the water absorption percentage and allowed the material structure to stabilize during testing. The presence of some compounds (with OH or NH functional groups) or elements (as salts or ions) in the extract interact with the chitosan matrix through hydrogen bonds or electrostatic forces, leading to a possible reduction of the interaction sites within the sponge structure and decreasing its absorption capacity in the aqueous medium. The last behavior was only observed in crosslinked biopolymers using physical, chemical, or enzymatic methods.[26,32] Other authors have also mentioned that interconnected pores and a macroscopically rough surface in the sponges facilitate the entry of external solvents into the network and contribute to faster absorption kinetics and high absorption capacity.[57]

2.5. Integration and Survival of *S. cerevisiae* into HAECa-Functionalized Chitosan Sponges. We performed growth kinetics and cell viability assays of *S. cerevisiae* to determine the optimal conditions for the integration process of the microorganism into the chitosan sponges. The exponential growth phase for yeast was observed in the interval time between 4 and 10 h of incubation. After 10 h, the yeast entered a stationary growth phase. To validate these data, cell viability was determined by the plate count method (number of colonies per

milliliter; CFU/mL). Yeast reached a maximum growth of 9×10^9 CFU/mL after 14 h of incubation; therefore, according to these results, approximately half of the yeast entered exponential phase at 8 h. At 8 h growth, the yeast showed optimal viable biomass (5×10^8 CFU/mL) for the integration process into the chitosan sponges. Moreover, the cells at 8 h are also found metabolically active, which is optimal for the integration process.

Yeast integration was carried out in an 8% v/v HAECa-functionalized chitosan sponge. This material was selected due to the characteristics presented as thermal stability, the optimal balance between porosity and water absorption, and the preservation of integrity and shape when exposed to water. In addition, at this concentration, the size pores within the sponge (6.81–9.95 μm) are very similar to the yeast size (5–10 μm), which we hypothesized would aid in the integration, growth, and colonization of microbial cells into the material. However, since the chitosan control sponge converted into a hydrogel when it absorbed water, this complicated the integration of the yeasts. Concerning the 8% v/v HAECa-functionalized chitosan sponge, the adsorption and embedding of yeast cells were shown in electron micrographs (Figure 6). In these (Figure 6A–C), yeast
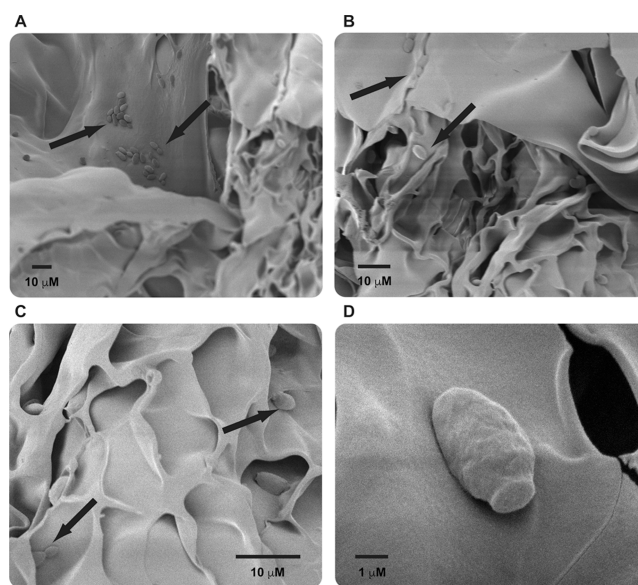
Figure 6. SEM micrographs of *S. cerevisiae* integration into chitosan sponges functionalized with 8% v/v of hydroalcoholic extract of *C. officinalis* (HAECa) flowers. (A) 600×, (B) 1000×, (C) 2000×, and (D) 10,000×.

cells appeared attached and stacked on the pores and the walls (marked with arrows) of the HAECa-functionalized chitosan sponges. Heterogeneous distribution of *S. cerevisiae* was observed within the material after the integration procedure. Figure 6D shows the conservation of yeast cell integrity after the process, which initially suggested the preservation of cell viability and metabolic capacity.

We next quantify the uptake and integration of *S. cerevisiae* into 8% v/v HAECa-functionalized chitosan sponges; the results showed that 58.34% of the viable cells initial (6×10^8 CFU/mL) were integrated into the material. The cell viability of the adsorbed yeast into the HAECa-functionalized chitosan sponge was determined after 6 and 12 h of the integration process using methylene blue staining. Between 57 and 58% of viable cell within the sponges was conserved at both monitoring times. Moreover, as can be observed in Figure 7, the cell viability of *S.*

cerevisiae did not present a statistical difference between the initial (0 h) and the 6 and 12 h post-integration times.
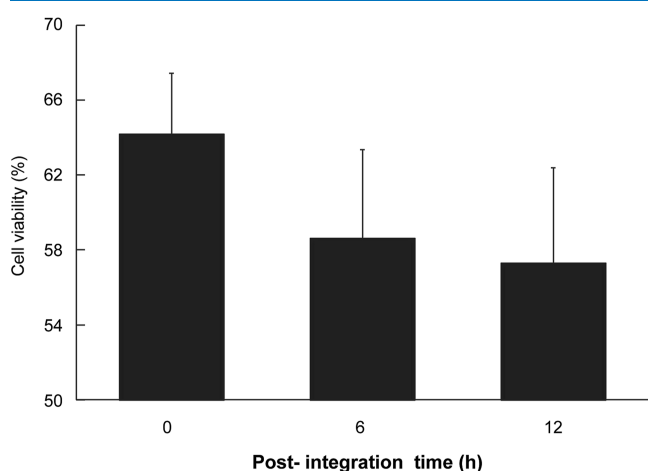
Figure 7. Cell viability of *S. cerevisiae* into HAECa-functionalized chitosan sponges at different post-integration times.

The integration percentage of *S. cerevisiae* viable cells (58.34%) attribute to the stirring conditions used in the process. The stationary phase (6 h) could induce the integration of a minor number of cells due to their tendency to flocculate.[58] Some authors suggest that stirring could generate conditions for mass transfer to submerged biomass, an increment of total biomass population, that cells in suspension had more contact time with the material and cause the increase in the number of integrated cells.[59,60] The amount of interstitial biomass plays a vital role in potential integrated biomass for the continuous adsorption−desorption equilibrium.[59] Another explanation of this phenomenon lies in the affinity of microbial cells for the material.

Concerning the last, cell integration depends on the cell loading and the specific characteristics of the support material.[61] These characteristics include surface charges, surface morphology, and surface area.[61−63] Yeast cells have negatively charged surfaces and could interact with the support material through electrostatic forces, becoming the principal adsorption mechanism for the cells.[61,64] The HAECa-functionalized chitosan sponge has elements such as K, Na, Cl, and Mg, which could develop surface charges in the material (considering that an acidic medium was used in its preparation) and are essential micronutrients that aid in the viability preservation of microorganisms.[65,66] In the entrapment method, the relation between support pore size and cell size is a critical parameter since, if the material pore size is larger than the microbial cells, this can cause the migration or leak of these into the environment.[67] On the other hand, a highly porous surface allows microorganisms to form biofilms, which is very important for an efficient integration process via adsorption in preformed membranes and sponges.[68−70] In the present study, the porosity (89.37%) and the pore size of 6.81−9.95 μm (like the size of *S. cerevisiae* of 5−10 μm) providing the material with the appropriate morphology and surface area conditions for an efficient integration process.

The percentage of cell viability that *S. cerevisiae* conserved into HAECa-functionalized chitosan sponges in the post-integration time is considered relevant due to the storage conditions evaluated in the synthetic-living material. The absence of nutrients can affect the growth rate and survival of the microorganisms due to their impact on metabolic activity.[71,72] Few studies about monitoring cell viability post-integration in material exist because this process is realized before subjecting the microorganism to a biocatalytic process.[73] Regarding using chitosan materials to integrate microorganisms, some authors have reported up to 66% of lactic acid bacteria at the end of the integration process onto chemically cross-linked chitosan beads.[74] In other biological systems, immobilized into chitosan beads have also been reported 71−76% for *Scenedesmus* sp. and 46% for *Saccharomyces obliquus*.[75] These results indicate that the percentage of cell viability after the integration process is dependent on the biological system, the shape, and characteristics of the chitosan material used in the process.

Considering the storage conditions used in the present study, the optimal integration of yeast cells into HAECa-functionalized chitosan sponges and the quick adaptation of the microorganism to the new environment played a relevant and critical role in viability conservation and survival. The above depended mainly on the sponge characteristics and the cell yeast/sponge interaction. Concerning the material characteristics, the addition of the HAECa introduced the elements K, Cl, Na, Mg, and other compounds (saccharides and antioxidants) onto the chitosan matrix could be contributed to the viability conservation of the yeast. Authors mentioned that cations K^+, Na^+, Mg^+, and the anion Cl^- are involucrate in generating and maintaining electrical gradients and electrochemical potentials in the cell membrane of the microorganisms, therefore in the homeostasis.[76−78]

The SEM micrographs (Figure 6A−C) confirm that the biological system was integrated into the synthetic material, confirming the production of a vita material. Also demonstrate the integrity in the cell wall of *S. cerevisiae* and a cell division process (Figure 6C,D), which could indicate a high probability of the conservation of its metabolic activity. The micrographs show that the yeast cells were attached to the material following different patterns. Lonely cells hosted into the pores of the sponge can be observed, and cell aggregates in the walls of the pores. Some authors have mentioned that microorganisms possess as adaptation and survival mechanisms to a new environment the formation of biofilms, which are expressed when integrated onto a surface by adsorption.[11] The last behavior has been observed in other studies.[68]

2.6. Biocatalytic Applications of the Vita Material Composed of *S. cerevisiae* Integrated into HAECa-Functionalized Chitosan Sponges. The first parameter tested was glucose consumption, a parameter related to the preservation of the biocatalytic capacity of *S. cerevisiae* integrated into the HAECa-functionalized chitosan sponges (8% v/v) under two post-integration times using as a control a free system (yeast without the integration process). Glucose consumption (for 2 consecutive days) was monitored in the vita material and compared with the glucose consumption in non-immobilized yeast cells cultured in a liquid medium. The results show that consumption of the microorganism integrated into the HAECa-functionalized chitosan sponges (both 0 and 7 days post-integration) showed an increased variability compared to the liquid culture without statistical significance between the three systems (Figure 8A). Moreover, there was more variability for the second day with respect to the first day within the vita material (Figure 8A). The above variability could be attributed to the quantity, density, and activity of viable cells within the material, the uniformity in their distribution, and their adaptation to the fermentation medium. A previous study
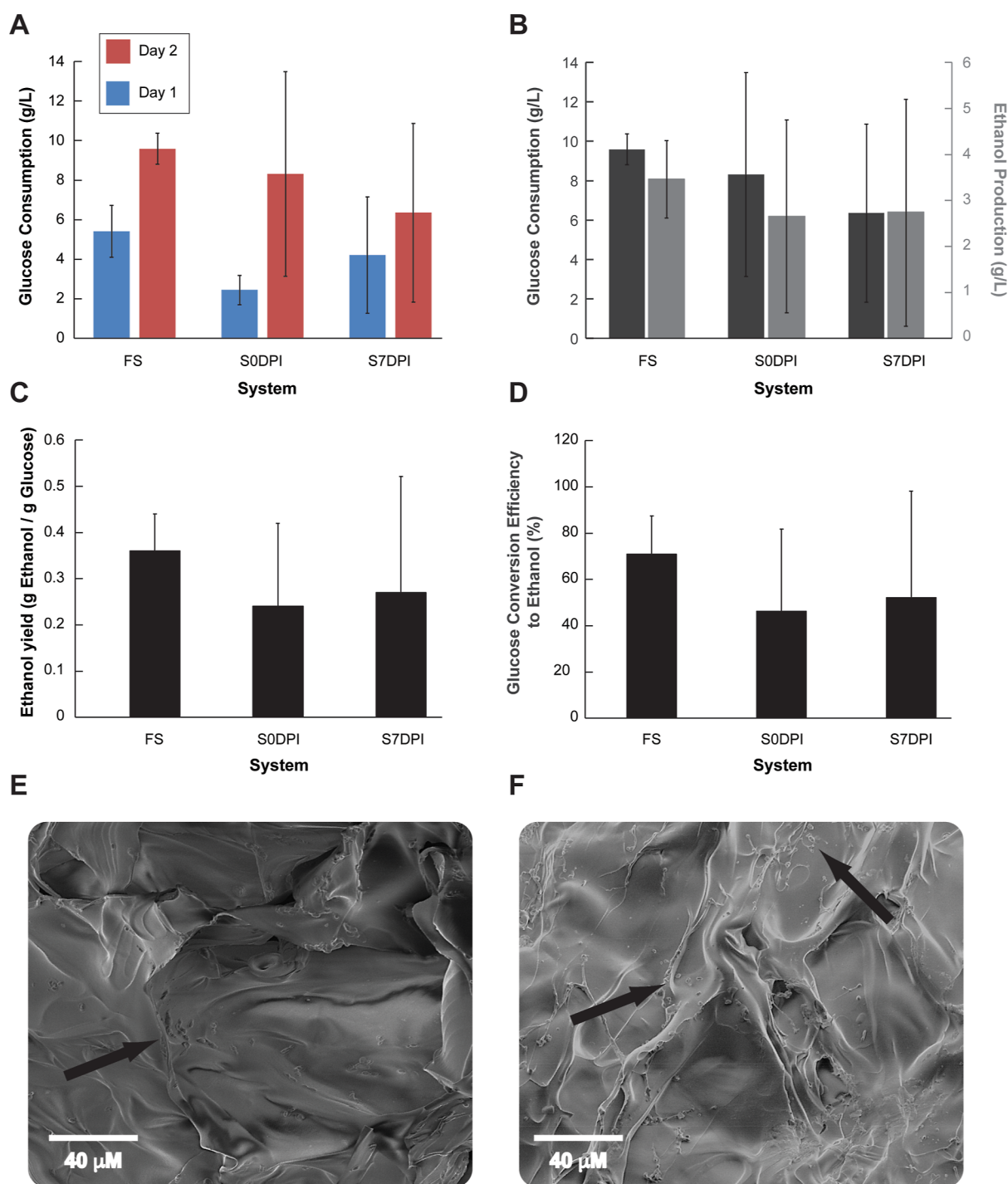
Figure 8. Biocatalytic behavior and morphology of *S. cerevisiae* into HAECa-functionalized chitosan sponges in the fermentation process (A) glucose consumption in three systems. FS corresponds to a non-immobilized liquid yeast culture, and S0DPI and S7DPI correspond to vita materials composed of HAECa-functionalized chitosan sponges after 0 and 7 days of immobilization of *S. cerevisiae*, respectively. Blue bars correspond to 1 day post-fermentation and red bars report 2 days post-fermentation. B−D report at 2 days after fermentation: (B) glucose consumption vs ethanol production. (C) Ethanol yield. (D) Glucose conversion efficiency to ethanol. (E) *S. cerevisiae* morphology before the fermentation process. (F) *S. cerevisiae* morphology after 2 days of the fermentation process.

showed that high cell densities, high cell activity, and a good mass transfer induce stable operation and high glucose consumption and ethanol productivity.[79]

The second parameter to determine the bioactivity of *S. cerevisiae* within the vita material was ethanol production (at day 2) from the consumption of glucose (Figure 8B); and its performance was compared to non-immobilized yeast cells in

liquid culture. In accordance with the variability in glucose consumption (Figure 8A), the systems with the integrated yeast presented a higher variability than the liquid non-immobilized culture (Figure 8B). However, ethanol production showed no significant differences between the three systems. Furthermore, we report ethanol yield (Figure 8C) and glucose conversion efficiency to ethanol (Figure 8D). The results show variability
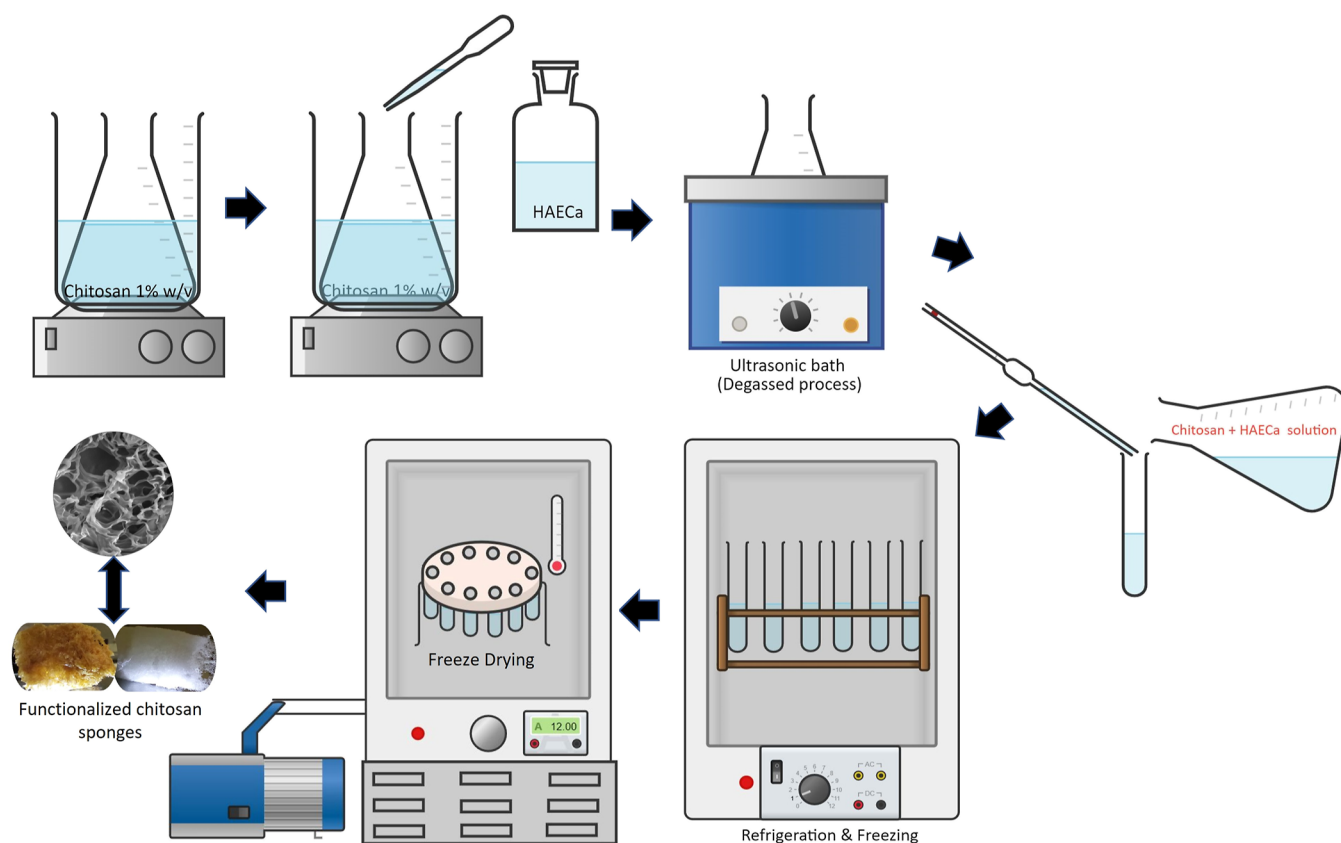
Figure 9. Scheme to produce HAECa-functionalized chitosan sponges.

within the three systems but show no significant difference and range between 0.35 and 0.28 g of ethanol produced per g of glucose (Figure 8C). Moreover, we observe a glucose conversion to ethanol within the systems between 45 and 70% (Figure 8D).

The micrographs of the material with *S. cerevisiae* before (Figure 8E) and after (Figure 8F) the fermentation process show a heterogeneous distribution and low cell densities of the yeast in the material. The yeast morphology matches that of a healthy cell, but this does not mean that *S. cerevisiae* metabolically has undergone any changes after the integration process and storage time.

The ethanol yield (0.36 ± 0.08) and glucose conversion efficiency to ethanol (70.80%) of the non-immobilized liquid yeast cell culture were similar to the control used in the literature (0.39 ± 0.02 and 77.2%) to compare with *S. cerevisiae* immobilized on membranes based on polyethyleneimine grafted collagen fiber evaluated.[79] The values of these parameters in the present study (Figure 8C,D) were lower than the membranes (0.46 ± 0.01 and 89.90%). In another study, *S. cerevisiae* (thermotolerant strain) immobilized on alginate-loofah sponges exhibited ethanol yield values (0.38 ± 0.01) lower than the non-immobilized cells (0.44 ± 0.01),[80] a behavior also observed in our study. Some authors mentioned that the immobilized yeast might use the sugar to synthesize other metabolites under stress conditions, such as saturated fatty acids, glycerol, or trehalose, so the glucose consumed is not only destined for the metabolic pathway of ethanol production.[81]

3. CONCLUSIONS

The present study achieved the integration of *S. cerevisiae* cells onto HAECa-functionalized chitosan sponges and the maintenance of viability post-integration process under limiting storage conditions (nutrients and temperature). We can affirm that a synthetic-living material (vita material) was obtained with potential use as a biocatalyst in diverse areas such as the food, pharmaceutical, biomedical, and energy sectors. Knowing the conservation of its biocatalytic activity post-integration process is also very important for future applications. In this sense, the glucose consumption and ethanol production of *S. cerevisiae* integrated onto HAECa-functionalized chitosan sponges in the fermentation process shows the conservation of its biocatalytic activity after the integration process. The variability in the behavior of *S. cerevisiae* integrated into the material can be improved for this specific application; however, the results here exhibited provide an interesting proof of concept on the synthesis of materials that integrate a synthetic and living part to enhance their properties. Our results demonstrate the ability to use biochemically modified chitosan sponges to host living and metabolically active yeast and maintain its biocatalytic capacity. Another aim of our future research line is to keep developing synthetic materials that can accommodate living systems of greater complexity, such as co-cultures, consortia of microorganisms, and phages, to be used for various applications in future endeavors.

4. EXPERIMENTAL SECTION

4.1. Chemicals. Medium molecular weight Chitosan with 75−85% deacetylated degree (Sigma-Aldrich batch STBH6274) and viscosity 200−800 Cp (Brookfield, at 1% w/

v in 2% v/v acetic acid at 25 °C). Acetic acid (ACS reagent 99.70%) Jalmek batch 19-2908-14A09. Commercial fluid hydroalcoholic extract from *C. officinalis* flower production batch EFC039081018 acquired in REDSA S.A de C.V.

4.2. Preparation of Chitosan Sponges with HAECa. The chitosan sponges were prepared with a chitosan solution of 1% w/v in acetic acid 2% v/v and using a vacuum freeze-drying method.[36] The hydroalcoholic extract of *C. officinalis* flower (HAECa) was added to chitosan solution in concentrations of 8, 10, and 12% v/v at room temperature. The chitosan solution with the extract was degassed in an ultrasonic bath for 4 min and deposited into plastic conical tubes (4.5 mL). These were refrigerated for 2 h at 4 °C and froze at −20 °C for 16 h. The chitosan sponges were obtained by lyophilizing (Christ alpha 1− 2 LD plus model freeze dryer) at −61 °C for 16 h (Figure 9). Also, a chitosan sponge control (only chitosan) was prepared as described above.

4.3. Physicochemical Characterization of HAECa-Functionalized Chitosan Sponges. SEM with chemical analysis by EDS: an Environmental Scanning Electron Microscope PHILIPS XL-30 model coupled to an energy-dispersive spectrometer EDAX Ametek was used to analyze the morphology and elemental composition of the chitosan sponge control and chitosan sponge functionalized with HAECa. Parts of the sponges were mounted on nickel stubs and coated with a layer of gold. In the morphological analysis, the samples were examined using 10 kV of accelerating voltage, and in the elemental composition, a voltage of 25 kV was used. The images were obtained by detector secondary electrons under high vacuum, magnifications of 50, 200, 500, and 1000×. The pore size was measured in the micrographs at 1000× resolutions and the average pore size was calculated from 200 measurements in diverse regions of the material. 200 measurements were obtained for each treatment and the control.

4.3.1. FTIR Analysis. FTIR spectrophotometer model NEXUS 670 from Thermo Nicolet was used to observe the changes in the chitosan matrix after the functionalization process with HAECa. A resolution of 4 cm^{-1} was used, and an average of over 64 scans in the range of 4000−650 cm^{-1}. The spectrum of the sponge functionalized with HAECa was obtained by an attenuated total reflection technique.[36]

4.3.2. Thermal Analyses. In the DSC test, the specimens were mounted in aluminum pans and heated from 25 to 400 °C using a heating rate of 10 °C/min under a nitrogen atmosphere on a DSC equipment Discovery series (TA Instruments).

4.3.3. Density. The density (ρ) of the sponge was calculated by measuring the weights and volumes of the samples.[82,83] An analytical balance was used to determine the weights (M) of the sponges, while the volumes (V) of the sponges were determined using a digital micrometer at three different positions. The densities of the sponges were calculated according to the following equation and expressed in g cm^{-3}.

$$\rho = M/V$$

4.3.4. Porosity. The determination of the porosity percent was carried out following the liquid displacement method using ethanol.[84] The chitosan sponge was immersed in a cylinder containing a known volume of ethanol (V_1). The total volume of ethanol and the chitosan sponge impregnated with ethanol was recorded as V_2. The chitosan sponge impregnated with ethanol was removed from the cylinder and the residual ethanol volume was recorded as V_3. The porosity of the chitosan sponge was expressed as

$$\% \text{ porosity} = [(V_1 - V_3)/(V_2 - V_3)] \times 100$$

4.3.5. Water Absorption. The determination of the water absorption capacity of the chitosan sponge control and functionalized with HAECa was achieved following a gravimetric method.[56] At different time intervals, the monitoring was from 1 h to 4 h in deionized water at room temperature. All sponges were weighed (W_1) and then immersed into deionized water, the wet sponges were weighted (W_2) at each interval, and the excess amount of water was removed using tissue paper. The percentage of water absorption was calculated using eq 1. The results were expressed as the mean ± standard deviation ($n = 3$).

$$\% \text{ water absorption} = [(W_2 - W_1)/(W_1)] \times 100 \qquad (1)$$

4.4. Integration of *S. cerevisiae* into HAECa-Functionalized Chitosan Sponges. *4.4.1. Yeast Strain and Maintenance.* The yeast *S. cerevisiae* CDBB-L-331 was obtained from the National Collection of Microbial Strains and Cell Culture at CINVESTAV-IPN, Zacatenco Unit. The cultures were maintained on Yeast Mold (YM BD Bioxon) agar and Yeast Peptone Dextrose (YPD MDC lab) broth and agar at 28 °C.

4.4.2. Growth Curve and Cell Viability by Plate Count Method. A pre-inoculum of *S. cerevisiae* was prepared in 10 mL of YPD broth and incubated at 28 °C and 150 rpm for 24 h. The growth curve of *S. cerevisiae* was determined by the inoculation of 10 mL of culture into 100 mL of YPD broth. The cultures were incubated at 28 °C at 150 rpm. At 0, 2, 4, and every 2 h until 14 h, monitoring was done by optical density and cell count analysis. The absorbance was read at 600 nm. The cell count was performed by spreading the sample onto YPD agar. The plates were incubated at 28 °C for 24 h, and then, the numbers of colonies were counted. Experiments were performed in triplicates ($n = 3$).

*4.4.3. Integration Process of *S. cerevisiae*.* Fresh inoculum of *S. cerevisiae* was prepared in YPD broth and incubated at 28 °C and 150 rpm. At 4, 6, and 8 h of growth, an aliquot was taken, and the absorbance was measured at 600 nm. At 8 h of growth (half of the exponential phase), 6 mL of the culture was taken and divided into sterile Eppendorf tubes (1 mL/tube). The tubes were centrifuged at 10,000 rpm for 5 min. The supernatant was discarded, and the cell pellet was washed with 1 mL of 0.85% sodium chloride using the conditions previously described. Finally, the cell pellet was reconstituted in 1 mL of 0.85% sodium chloride.

Functionalized sponges were sterilized by UV light for 30 min and then placed into sterile conical tubes. Subsequently, 3 mL of the *S. cerevisiae* suspension was added to each tube until functionalized sponge was completely covered. Tubes were incubated at 28 °C with no shaking for 6 h and then at 150 rpm for another 6 h (total integration time of 12 h). The sterility test of sponges was evaluated using YPD broth. The percentage integration of viable yeast cells was evaluated by the plate count method using YPD agar through culture cell count before and after the integration process.

*4.4.4. SEM of *S. cerevisiae* Integrated.* SEM was used to observe the morphology of *S. cerevisiae* integrated and adhered into the HAECa-functionalized chitosan sponge. For this purpose, samples from the viability test corresponding at 12 h post-integration process was used. The sponge samples were dehydrated with the increase in ethanol concentrations (50, 70, 90, and 100%) for 15 min. Afterward, the samples were placed with tweezers in a sample holder soaked in ethanol. Then, the sample holder was submitted to a critical point drying process

(equipment Quorum K850 model) for 1 h using a pressure of 1100 psi. The samples were fixed on stubs of carbon tape of double-sided fixed previously on a sample holder. Finally, the samples were coated with a layer of gold through a metallization process (equipment Quorum Q150R ES model). *S. cerevisiae* cells integrated into functionalized chitosan sponge were observed using a field emission scanning electron microscope JEOL JSM-6390LV model (Tokyo, Japan). The images were obtained by a SEI detector, under high vacuum, 1 kV of voltage with a working distance of approximately 7 mm and magnifications 600×, 1000×, 2000×, and 10,000×.

4.5. Viability Assessment of *S. cerevisiae* Integrated into HAECa-Functionalized Chitosan Sponges. After completing the integration time, the sponges were transferred into new sterile conical tubes and maintained at 4 °C without a medium culture. The absorbance of the remaining solution was measured at 600 nm using 0.85% NaCl solution as blank. The yeast viability was evaluated by methylene blue staining and the plate count method. 6 and 12 h post-processing, the tubes containing the *S. cerevisiae* integrated to HAECa-functionalized chitosan sponges were taken out of the refrigerator. Three milliliters of 1× phosphate-buffered saline (PBS) was added to each tube and vortexed for 1 min. The absorbance of the remaining solution was again measured at 600 nm, and cell viability was evaluated by methylene blue staining.

Cell viability by methylene blue staining: a methylene blue solution (final concentration of 0.1 mg/mL) was prepared with 2% sodium citrate dihydrate. The *S. cerevisiae* viability was analyzed on a hemocytometer by optical microscopy at 6 and 12 h post-processing. Live cells will be colorless, while dead cells will appear dark blue. The result was expressed as a percentage of viability which was calculated based on the cell count (viable and non-viable cells) in four fields under a microscope.

4.6. Biocatalytic Capacity of *S. cerevisiae* Integrated into HAECa-Functionalized Chitosan Sponges. The biocatalytic capacity of *S. cerevisiae* once integrated into HAECa-functionalized chitosan sponges was tested through the production of ethanol from glucose. For this purpose, a fermentation medium, *S. cerevisiae* integrated into the material with two post-integration times (0 and 7 days) was available. The parameters monitored were glucose consumption (as residual reducing sugars in the fermentation medium) and ethanol production (potassium dichromate method adapted to microtiter plates), also ethanol yield, and glucose conversion efficiency to ethanol were calculated. As a control, *S. cerevisiae* in liquid medium was used.

4.6.1. Fermentation Medium. The fermentation medium was prepared with 19 g L^{-1} of D-glucose and 1 g/L^{-1} of yeast extract in distilled water, and a volume of 100 mL was deposited in Erlenmeyer flasks (capacity of 250 mL), and then, it was placed autoclave for the sterilization process (120 °C for 15 min).

4.6.2. Inoculation of Fermentation Medium. In Erlenmeyer flasks with fermentation medium were deposited *S. cerevisiae* integrated into HAECa-functionalized chitosan sponges previously prepared using two post-integration times (0 and 7 days). As a control, an inoculum (1 mL) of the yeast without integration (free system) previously grew in a YPD medium and then incubated under the same integration conditions used in the functionalized chitosan sponges was used. The Erlenmeyer flasks were incubated at 28 °C and without agitation for 48 h. Each system was tested by duplicate and reproducibility was performed.

4.6.3. Preparation of Samples for the Determination of Reducing Sugars and Ethanol Production. The fermentation medium was collected after the process and centrifuged (12,000 rpm for 10 min) at 4 °C, and the supernatants were removed to fresh tubes for following analysis of reductor sugar (at 24 and 48 h of fermentation process) and ethanol production at 48 h of process. The analysis was realized by duplicate.

4.6.4. Reducing Sugar Determination. The glucose consumption of *S. cerevisiae* coupled to HAECa-functionalized chitosan sponges was determined as reducing sugars by the adapted method of dinitrosalicylic acid (DNS) to microtiter plates.[85] The reaction was carried out in microtubes of 1.5 mL, adding 25 μL of the sample or distilled water (blank) to 25 μL of DNS reagent. Subsequently, to perform the reaction, the microtube with a cap was placed in a thermomixer (Eppendorf) to 100 °C for 5 min; then, 250 μL of frozen distilled water was immediately added to each microtube. After the content of the microtubes was deposited in the wells of a microtiter plate, then the absorbance was measured to 540 nm in a microplate spectrophotometer (Thermo Scientific Multiskan GO). According to the last procedure, the calibration curve with glucose (from dilutions of standard solution of 10 g/L) also was obtained. The calculation of glucose consumption was obtained by subtracting the concentration of reducing sugars remaining in the fermentation medium from the initial glucose concentration.

4.6.5. Ethanol Production. The ethanol produced for *S. cerevisiae* was determined by the potassium dichromate method[86] adapted to microtiter plates. For this purpose, used potassium dichromate solution prepared with sulfuric acid, and the fermentation medium previously centrifuged was distilled. In microtubes of 1.5 mL were deposited 100 μL of the sample or distilled water (blank) and a volume of 200 μL of potassium dichromate solution, and then, the microtubes were homogenized. These were incubated at room temperature and darkness for 15 min. Subsequently, 500 μL of distilled water was dispensed in microtubes, and these were homogenized again. A volume of 300 μL was deposited in the microtiter plate, and the absorbance was measured to 585 nm in a microplate spectrophotometer (Thermo Scientific Multiskan GO). According to the last procedure, the calibration curve from dilutions of standard ethanol solution (20 g/L) also was obtained. The ethanol yield (ratio of the ethanol produced to the total glucose utilized) and glucose conversion efficiency to ethanol (ratio of ethanol yield to the theoretical value of ethanol yield) were calculated from values of glucose consumption (g L^{-1}), ethanol production (g L^{-1}), and theoretical value of ethanol yield (0.51 g/g).

4.7. Statistical Analysis. Results of porosity, water absorption, immobilization percentage, viability percentage, glucose consumption, ethanol production, ethanol yield, and glucose conversion efficiency to ethanol were presented as the mean ± standard deviation. The data were subjected to one-way analysis of variance (ANOVA) using STATGRAPHICS PLUS statistical program. Duncan's method was used in the multiple comparisons in the cases where the ANOVA detected a significant difference ($P < 0.05$).

■ ASSOCIATED CONTENT

Data Availability Statement

All the data obtained and materials analyzed in this research are available with the corresponding author.

■ AUTHOR INFORMATION

Corresponding Author

José R. Morones-Ramírez − *School of Chemistry, Autonomous University of Nuevo Leon (UANL), San Nicolas de los Garza, Nuevo Leon 66455, Mexico; Applied Microbiology Department, NanoBiotechnology Research Group, Research Center on Biotechnology and Nanotechnology, School of Chemical Sciences, Autonomous University of Nuevo Leon, PIIT, Apodaca, Nuevo Leon 66629, Mexico;* ⊙ orcid.org/0000-0001-7009-686X; Email: jose.moronesrmr@uanl.edu.mx

Authors

Isabel O. Caamal-Herrera − *School of Chemistry, Autonomous University of Nuevo Leon (UANL), San Nicolas de los Garza, Nuevo Leon 66455, Mexico; Applied Microbiology Department, NanoBiotechnology Research Group, Research Center on Biotechnology and Nanotechnology, School of Chemical Sciences, Autonomous University of Nuevo Leon, PIIT, Apodaca, Nuevo Leon 66629, Mexico*

Mariana B. Erreguin-Isaguirre − *School of Chemical Engineering Pharmaceutics, Technological University of San Juan del Rio, San Juan del Rio, Queretaro 76800, Mexico*

Angel León-Buitimea − *School of Chemistry, Autonomous University of Nuevo Leon (UANL), San Nicolas de los Garza, Nuevo Leon 66455, Mexico; Applied Microbiology Department, NanoBiotechnology Research Group, Research Center on Biotechnology and Nanotechnology, School of Chemical Sciences, Autonomous University of Nuevo Leon, PIIT, Apodaca, Nuevo Leon 66629, Mexico*

Complete contact information is available at:
https://pubs.acs.org/10.1021/acsomega.2c07847

Author Contributions

Conceptualization, I.O.C.-H. and J.R.M.-R.; acquisition, analysis, and interpretation of data, I.O.C.-H. and J.R.M.-R.; M.B.E.-I. assisted in the research work. A.L.-B. contributed to the research work and revised the manuscript. I.O.C.-H., A.L.-B., and J.R.M.-R. wrote the original draft preparation. All authors reviewed the final version of the manuscript.

Notes

The authors declare no competing financial interest.

■ ACKNOWLEDGMENTS

■ REFERENCES

(1) Le Feuvre, R. A.; Scrutton, N. S. A Living Foundry for Synthetic Biological Materials: A Synthetic Biology roadmap to New Advanced Materials. *Synth. Syst. Biotechnol.* **2018**, *3*, 105−112.

(2) Wondraczek, L.; Pohnert, G.; Schacher, F. H.; Köhler, A.; Gottschaldt, M.; Schubert, U. S.; Küsel, K.; Brakhage, A. A. Artificial Microbial Arenas: Materials for Observing and Manipulating Microbial Consortia. *Adv. Mater.* **2019**, *31*, 1900284.

(3) Nguyen, P. Q.; Courchesne, N. M.; Duraj-Thatte, A.; Praveschotinunt, P.; Joshi, N. S. Engineered Living Materials: Prospects and Challenges for Using Biological Systems to Direct the Assembly of Smart Materials. *Adv. Mater.* **2018**, *30*, 1704847.

(4) Schaffner, M.; Rühs, P. A.; Coulter, F.; Kilcher, S.; Studart, A. R. 3D Printing of Bacteria into Functional Complex Materials. *Sci. Adv.* **2017**, *3*, No. eaao6804.

(5) Prapagdee, B.; Wankumpha, J. Phytoremediation of Cadmium-polluted Soil by Chlorophytum laxum combined with Chitosan-immobilized Cadmium-resistant Bacteria. *Environ. Sci. Pollut. Res.* **2017**, *24*, 19249−19258.

(6) Santos, E.; Rostro-Alanís, I.; Parra-Saldívar, M.; Alvarez, R.; Álvarez, A. J. A Novel Method for Bioethanol Production using Immobilized Yeast Cells in Calcium-alginate films and Hybrid Composite Pervaporation Membrane. *Bioresour. Technol.* **2018**, *247*, 165−173.

(7) Silveira-Martins, S. C.; Martins, C. M.; Guedes-Fiúza, L. M. C.; Santaella, S. T. Immobilization of Microbial Cells: A Promising Tool for Treatment of Toxic Pollutants in Industrial Wastewater. *Afr. J. Biotechnol.* **2013**, *12*, 4412−4418.

(8) Bayat, Z.; Hassanshahian, M.; Cappello, S. Immobilization of Microbes for Bioremediation of Crude Oil Polluted Environments: A Mini Review. *Open Microbiol. J.* **2015**, *9*, 48−54.

(9) Gamarra, N. N.; Villena, G. K.; Gutiérrez-Correa, M. Cellulase Production by Aspergillus niger in Biofilm, Solid-state, and Submerged Fermentations. *Appl. Microbiol. Biotechnol.* **2010**, *87*, 545−551.

(10) Tam, S. K.; Dusseault, J.; Bilodeau, S.; Langlois, G.; Hallé, J. P.; Yahia, L. Factors Influencing Alginate Gel Biocompatibility. *J. Biomed. Mater. Res., Part A* **2011**, *98A*, 40−52.

(11) Żur, J.; Wojcieszyńska, D.; Guzik, U. Metabolic Responses of Bacterial Cells to Immobilization. *Molecules* **2016**, *21*, 958.

(12) Lajtai-Szabó, P.; Hülber-Beyer, E.; Nemestóthy, N.; Bélafi-Bakó, K. The Role of Physical Support in Secondary Metabolite Production by Streptomyces species. *Biochem. Eng. J.* **2022**, *185*, 108495.

(13) Miao, H.; Li, M.; Sun, X.; Xia, J.; Li, Y.; Li, J.; Wang, F.; Xu, J. Effects of Pore Size and Crosslinking Methods on the Immobilization of Myoglobin in SBA-15. *Front. Bioeng. Biotechnol.* **2022**, *9*, 827552.

(14) Gunathilake, T. U.; Ching, Y. C.; Ching, K. Y.; Chuah, C. H.; Abdullah, L. C. Biomedical and Microbiological Applications of Bio-based Porous Materials: A Review. *Polymers* **2017**, *9*, 160.

(15) Foster, L. J. R.; Ho, S.; Hook, J.; Basuki, M.; Marçal, H. Chitosan as a biomaterial: Influence of Degree of Deacetylation on its Physiochemical, Material and Biological Properties. *PLoS One* **2015**, *10*, No. e0135153.

(16) Zivanovic, S.; Chi, S.; Draughon, F. Antimicrobial Activity of Chitosan Films Enriched with Essential Oils. *J. Food Sci.* **2005**, *70*, M45−M51.

(17) Noel, S. P.; Courtney, H.; Bumgardner, J. D.; Haggard, W. O. Chitosan films: A Potential Local Drug Delivery System for Antibiotics. *Clin. Orthop. Relat. Res.* **2008**, *466*, 1377−1382.

(18) Shinonaga, M.; Kawamura, Y.; Yamane, T. Immobilization of Yeast Cells with Cross-linked Chitosan Beads. *J. Ferment. Bioeng.* **1992**, *74*, 90−94.

(19) Vimala, K.; Mohan, Y.; Sivudu, K.; Varaprasad, K.; Ravindra, S.; Reddy, N.; Padma, Y.; Sreedhar, B.; MohanaRaju, K. Fabrication of Porous Chitosan Films Impregnated with Silver Nanoparticles: A Facile Approach for Superior Antibacterial Application. *Colloids Surf., B* **2010**, *76*, 248−258.

(20) Gomes, S.; Rodrigues, G.; Martins, G.; Henriques, C.; Silva, J. C. Evaluation of Nanofibrous Scaffolds Obtained from Blends of Chitosan,

Gelatin and Polycaprolactone for Skin Tissue Engineering. *Int. J. Biol. Macromol.* **2017**, *102*, 1174−1185.

(21) Gomes, S. R.; Rodrigues, G.; Martins, G. G.; Roberto, M. A.; Mafra, M.; Henriques, C. M. R.; Silva, J. C. In vitro and in vivo Evaluation of Electrospun Nanofibers of PCL, Chitosan and Gelatin: A Comparative Study. *Mater. Sci. Eng., C* **2015**, *46*, 348−358.

(22) Annabi, N.; Nichol, J. W.; Zhong, X.; Ji, C.; Koshy, S.; Khademhosseini, A.; Dehghani, F. Controlling the Porosity and Microarchitecture of Hydrogels for Tissue Engineering. *Tissue Eng., Part B* **2010**, *16*, 371−383.

(23) Caamal-Herrera, I. O. *Elaboration and Characterization of Materials of Chitosan with Plant Extracts for Biomedical Application.* Ph.D. Thesis, Center for Research and Advanced Studies of the National Polytechnic Institute, Applied Physics Department. Mérida, Yucatán, México, 2018.

(24) Barragán-Menéndez, C.; Gálvez-López, D.; Rosas-Quijano, R.; Salvador-Figueroa, M.; Ovando-Medina, I.; Vázquez-Ovando, A. Films of Chitosan andAloe vera for Maintaining the Viability and Antifungal Activity of Lactobacillus paracasei TEP6. *Coatings* **2020**, *10*, 259.

(25) Ramos, C. L.; de Figueiredo Vilela, L.; Schwan, R. F. Genetic Engineering as a Driver for Biotechnological Developments and Cloning Tools to Improve Industrial Microorganisms. In *Bioprocessing for Biomolecules Production*, 1st ed.; Wiley, 2020; pp 275−280.

(26) Dilarri, G.; Corso, C. R. Saccharomyces cerevisiae Immobilized onto Cross-linked Chitosan Beads: Application of a Novel Material for the Removal of Dye Toxicity. *Environ. Technol.* **2018**, *39*, 1851−1867.

(27) Garg, T.; Chanana, A.; Joshi, R. Preparation of Chitosan Scaffolds for Tissue Engineering using Freeze Drying Technology. *IOSR J. Pharm.* **2012**, *2*, 72−73.

(28) Freeman, A.; Dror, Y. Immobilization of ″Disguised″ Yeast in Chemically Crosslinked Chitosan beads. *Biotechnol. Bioeng.* **1994**, *44*, 1083−1088.

(29) Arunraj, B.; Talasila, S.; Rajesh, V.; Rajesh, N. Removal of Europium from Aqueous Solution usingSaccharomyces cerevisiae Immobilized in Glutaraldehyde Cross-linked Chitosan. *Separ. Sci. Technol.* **2019**, *54*, 1620−1631.

(30) Suica-Bunghez, I. R.; Ion, R. M. Complex Spectral Characterization of Active Principles from Marigold (Calendula Officinalis). *J. Sci. Arts* **2011**, *11*, 59−64.

(31) Suderman, N.; Isa, M. I. N.; Sarbon, N. M. The Effect of Plasticizers on the Functional Properties of Biodegradable Gelatin-based Film: A review. *Food Biosci.* **2018**, *24*, 111−119.

(32) Long, H.; Ma, K.; Xiao, Z.; Ren, X.; Yang, G. Preparation and Characteristics of Gelatin Sponges Crosslinked by Microbial Trans-glutaminase. *PeerJ* **2017**, *5*, No. e3665.

(33) Wang, X.; Lou, T.; Zhao, W.; Song, G.; Li, C.; Cui, G. The Effect of Fiber Size and Pore Size on Cell Proliferation and Infiltration in PLLA Scaffolds on Bone Tissue Engineering. *J. Biomater. Appl.* **2016**, *30*, 1545−1551.

(34) Lien, S. M.; Ko, L. Y.; Huang, T. J. Effect of Pore Size on ECM Secretion and Cell Growth in Gelatin Scaffold for Articular Cartilage Tissue Engineering. *Acta Biomater.* **2009**, *5*, 670−679.

(35) Cai, S. J.; Li, C. W.; Weihs, D.; Wang, G. J. Control of Cell Proliferation by a Porous Chitosan Scaffold with Multiple Releasing Capabilities. *Sci. Technol. Adv. Mater.* **2017**, *18*, 987−996.

(36) Wang, M.; Ma, Y.; Sun, Y.; Hong, S. Y.; Lee, S. K.; Yoon, B.; Chen, L.; Ci, L.; Nam, J. D.; Chen, X.; Suhr, J. Hierarchical Porous Chitosan Sponges as Robust and Recyclable Adsorbents for Anionic Dye Adsorption. *Sci. Rep.* **2017**, *7*, 18054.

(37) Dai, M.; Zheng, X.; Xu, X.; Kong, X.; Li, X.; Guo, G.; Luo, F.; Zhao, X.; Wei, Y. Q.; Qian, Z. Chitosan-alginate Sponge: Preparation and Application in Curcumin Delivery for Dermal Wound Healing in Rat. *J. Biomed. Biotechnol.* **2009**, *2009*, 595126.

(38) Ikeda, T.; Ikeda, K.; Yamamoto, K.; Ishizaki, H.; Yoshizawa, Y.; Yanagiguchi, K.; Yamada, S.; Hayashi, Y. Fabrication and Characteristics of Chitosan Sponge as a Tissue Engineering Scaffold. *BioMed Res. Int.* **2014**, *2014*, 786892.

(39) Jiang, X.; Jiang, T.; Gan, L.; Zhang, X.; Dai, H.; Zhang, X. The Plasticizing Mechanism and Effect of Calcium Chloride on Starch/poly(vinyl alcohol) Films. *Carbohydr. Polym.* **2012**, *90*, 1677−1684.

(40) Hirase, R.; Higashiyama, Y.; Mori, M.; Takahara, Y.; Yamane, C. Hydrated Salts as both Solvent and Plasticizer for Chitosan. *Carbohydr. Polym.* **2010**, *80*, 993−996.

(41) Nguyen, V. C.; Nguyen, V. B.; Hsieh, M. F. Curcumin-Loaded Chitosan/Gelatin Composite Sponge for Wound Healing Application. *Int. J. Polym. Sci.* **2013**, *2013*, 106570.

(42) Nainggolan, I.; Shantini, D.; Nasution, T. I.; Derman, M. N. Role of Metals Content in Spinach in Enhancing the Conductivity and Optical Band Gap of Chitosan Films. *Adv. Mater. Sci. Eng.* **2015**, *2015*, 702815.

(43) Andersen, F. A.; Bergfeld, W. F.; Belsito, D. V.; Hill, R. A.; Klaassen, C. D.; Liebler, D. C.; Marks, J. G., Jr.; Shank, R. C.; Slaga, T. J.; Snyder, P. W. Final Report of the Cosmetic Ingredient Review Expert Panel Amended Safety Assessment of Calendula officinalis-derived Cosmetic Ingredients. *Int. J. Toxicol.* **2010**, *29*, 221S−243S.

(44) Fernandes Queiroz, M.; Melo, K. R.; Sabry, D. A.; Sassaki, G. L.; Rocha, H. A. Does the use of chitosan contribute to oxalate kidney stone formation? *Mar. Drugs* **2014**, *13*, 141−158.

(45) Neto, C. G. T.; Giacometti, J. A.; Job, A. E.; Ferreira, F. C.; Fonseca, J. L. C.; Pereira, M. R. Thermal Analysis of Chitosan Based Networks. *Carbohydr. Polym.* **2005**, *62*, 97−103.

(46) Lozano-Navarro, J. L.; Díaz-Zavala, N. P.; Velasco-Santos, C.; Melo-Banda, J. A.; Páramo-García, U.; Paraguay-Delgado, F.; García-Alamilla, R.; Martínez-Hernández, A. L.; Zapién-Castillo, S. Chitosan-Starch Films with Natural Extracts: Physical, Chemical, Morphological and Thermal Properties. *Materials* **2018**, *11*, 120.

(47) Altiok, D.; Altiok, E.; Tihminlioglu, F. Physical, Antibacterial and Antioxidant Properties of Chitosan Films Incorporated with Thyme Oil for Potential Wound Healing Applications. *J. Mater. Sci.: Mater. Med.* **2010**, *21*, 2227−2236.

(48) Dong, Y.; Ruan, Y.; Wang, H.; Zhao, Y.; Bi, D. Studies on Glass Transition Temperature of Chitosan with Four Techniques. *J. Appl. Polym. Sci.* **2004**, *93*, 1553−1558.

(49) Neto, C. G. T.; Giacometti, J. A.; Job, A. E.; Ferreira, F. C.; Fonseca, J. L. C.; Pereira, M. R. Thermal, Analysis of Chitosan Based Networks. *Carbohydr. Polym.* **2005**, *62*, 97−103.

(50) Rodríguez-Núñez, J. R.; Madera-Santana, T. J.; Sánchez-Machado, D. I.; López-Cervantes, J.; Soto-Valdez, H. Chitosan/Hydrophilic Plasticizer-Based Films: Preparation, Physicochemical and Antimicrobial Properties. *J. Polym. Environ.* **2014**, *22*, 41−51.

(51) Lemes, B. M.; Novatski, A.; Ferrari, P. C.; Minozzo, B. R.; Justo, A. D. S.; Petry, V. E. K.; Vellosa, J. C. R.; Sabino, S. D. R. F.; Gunha, J. V.; Esmerino, L. A.; Beltrame, F. L. Physicochemical, Biological and Release Studies of Chitosan Membranes Incorporated with Euphorbia umbellata Fraction. *Rev. Bras. Farmacogn.* **2018**, *28*, 433−443.

(52) Dai, Z.; Ronholm, J.; Tian, Y.; Sethi, B.; Cao, X. Sterilization Techniques for Biodegradable Scaffolds in Tissue Engineering Applications. *J. Tissue Eng.* **2016**, *17*, 204173141664881.

(53) Szymańska, E.; Winnicka, K. Stability of Chitosan a Challenge for Pharmaceutical and Biomedical Applications. *Mar. Drugs* **2015**, *13*, 1819−1846.

(54) Attawia, M. A.; Herbert, K. M.; Uhrich, K. E.; Langer, R.; Laurencin, C. T. Proliferation, Morphology, and Protein Expression by Osteoblasts Cultured on Poly (anhydride-co-imides). *J. Biomed. Mater. Res.* **1999**, *48*, 322−327.

(55) She, Z.; Zhang, B.; Jin, C.; Feng, Q.; Xu, Y. Preparation and in vitro degradation of porous three-dimensional silk fibroin/chitosan scaffold. *Polym. Degrad. Stabil.* **2008**, *93*, 1316−1322.

(56) Anbazhagan, S.; Thangavelu, K. P. Application of Tetracycline Hydrochloride Loaded-fungal Chitosan and Aloe vera Extract Based Composite Sponges for Wound Dressing. *J. Adv. Res.* **2018**, *14*, 63−71.

(57) Pan, Y.; Shi, K.; Liu, Z.; Wang, W.; Peng, C.; Ji, X. Synthesis of a New Kind of Macroporous Polyvinyl-alcohol Formaldehyde based Sponge and its Water Superabsorption Performance. *RSC Adv.* **2015**, *5*, 78780−78789.

(58) Soares, E. Flocculation inSaccharomyces cerevisiae: A Review. *J. Appl. Microbiol.* **2011**, *110*, 1−18.

(59) de Ory, I.; Cabrera, G.; Ramirez, M.; Blandino, A. Immobilization of Enzymes and Cells. In *Immobilization of Cells on Polyurethane Foam*; *Methods in Biotechnology*; Humana Press, 2006; Vol. 22, pp 357−365.

(60) Milessi, T. S.; Antunes, F. A.; Chandel, A. K.; da Silva, S. S. Hemicellulosic Ethanol Production by Immobilized Cells of Scheffersomyces stipitis: Effect of Cell Concentration and Stirring. *Bioengineered* **2015**, *6*, 26−32.

(61) Zhu, D.; Li, X.; Liao, X.; Shi, B. Immobilization ofSaccharomyces cerevisiae using Polyethyleneimine Grafted Collagen Fiber as Support and Investigations of its Fermentation Performance. *Biotechnol. Biotechnol. Equip.* **2018**, *32*, 109−115.

(62) Kilonzo, P.; Margaritis, A.; Bergougnou, M. Effects of Surface Treatment and Process Parameters on Immobilization of Recombinant Yeast Cells by Adsorption to Fibrous Matrices. *Bioresour. Technol.* **2011**, *102*, 3662−3672.

(63) Mustranta, A.; Pere, J.; Poutanen, K. Comparison of Different Carriers for Adsorption ofSaccharomyces cerevisiae and Zymomonas mobilis. *Enzym. Microb. Technol.* **1987**, *9*, 272−276.

(64) Van Haecht, J. L.; Bolipombo, M.; Rouxhet, P. G. Immobilization of Saccharomyces cerevisiae by Adhesion: Treatment of the Cells by Al Ions. *Biotechnol. Bioeng.* **1985**, *27*, 217−224.

(65) Dibrova, D. V.; Galperin, M. Y.; Koonin, E. V.; Mulkidjanian, A. Y. Ancient Systems of Sodium/Potassium Homeostasis as Predecessors of Membrane Bioenergetics. *Biochemistry* **2015**, *80*, 495−516.

(66) Dong-yeon, L. D.; Galera-Laporta, L.; Bialecka-Fornal, M.; Chae Moon, E.; Shen, Z.; Steven Briggs, S. P.; Garcia-Ojalvo, J.; GürolSüel, M. G. M. Magnesium Flux Modulates Ribosomes to Increase Bacterial Survival. *Cell* **2019**, *177*, 352−360.e13.

(67) Dzionek, A.; Wojcieszyńska, D.; Guzik, U. Natural Carriers in Bioremediation: A Review. *Electron. J. Biotechnol.* **2016**, *23*, 28−36.

(68) Dzionek, A.; Wojcieszyńska, D.; Hupert-Kocurek, K.; Adamczyk-Habrajska, M.; Guzik, U. Immobilization ofPlanococcus sp. S5 Strain on the Loofah Sponge and Its Application in Naproxen Removal. *Catalysts* **2018**, *8*, 176.

(69) Willaert, R. G. Fermentation Microbiology and Biotechnology. *Cell Immobilization and Its Applications in Biotechnology, Current Trends and Future Prospects*, 1st ed,; CRC Press, 2019; Chapter 17.

(70) Dang, H. T. T.; Dinh, C. V.; Nguyen, K. M.; Tran, N. T. H.; Pham, T. T.; Narbaitz, R. M. Loofah Sponges as Bio-Carriers in a Pilot-Scale Integrated Fixed-Film Activated Sludge System for Municipal Wastewater Treatment. *Sustainability* **2020**, *12*, 4758.

(71) Price, P. B.; Sowers, T. Temperature Dependence of Metabolic Rates for Microbial Growth, Maintenance, and Survival. *Proc. Natl. Acad. Sci.* **2004**, *101*, 4631−4636.

(72) Lempp, M.; Lubrano, P.; Bange, G.; Link, H. Metabolism of Non-growing Bacteria. *Biol. Chem.* **2020**, *401*, 1479−1485.

(73) Guliy, O. I.; Simakov, V. V.; Karavaeva, O. A.; Smirnov, A. V. Immobilization of Microbial Cells on Polymeric Matrices Modified by Plasma Treatment. *Appl. Biochem. Microbiol.* **2020**, *56*, 237−243.

(74) Le-Tien, C.; MilletteMateescu, M. M. A.; Lacroix, M. Modified Alginate and Chitosan for Lactic Acid Bacteria Immobilization. *Biotechnol. Appl. Biochem.* **2004**, *39*, 189.

(75) Fierro, S.; del Pilar Sánchez-Saavedra, M. P.; Copalcúa, C. Nitrate and Phosphate Removal by Chitosan Immobilized Scenedesmus. *Bioresour. Technol.* **2008**, *99*, 1274−1279.

(76) Benarroch, J. M.; Asally, M. The Microbiologist's Guide to Membrane Potential Dynamics. *Trends Microbiol.* **2020**, *28*, 304−314.

(77) Góral, M.; Pankiewicz, U. Effect of Pulsed Electric Fields (PEF) on Accumulation of Magnesium in Lactobacillus rhamnosus B 442 Cells. *J. Membr. Biol.* **2017**, *250*, 565−572.

(78) Jennings, M. L.; Cui, J. Chloride Homeostasis in Saccharomyces cerevisiae: High Affinity Influx V-ATPase-dependent Sequestration, and Identification of a Candidate Cl _ Sensor. *J. Gen. Physiol.* **2008**, *131*, 379−391.

(79) Zhu, D.; Xia, L.; Xuepin, L.; Bi, S. Immobilization of Saccharomyces cerevisiae using Polyethyleneimine grafted Collagen Fibre as Support and Investigations of its Fermentation Performance. *Biotechnol. Biotechnol. Equip.* **2018**, *32*, 109−115.

(80) Nuanpeng, S.; Thanonkeo, S.; Klanrit, P.; Thanonkeo, P. Ethanol Production from Sweet Sorghum by Saccharomyces cerevisiae DBKKUY-53 immobilized on Alginate-loofah Matrices. *Braz. J. Microbiol.* **2018**, *49*, 140−150.

(81) Yu, J.; Zhang, X.; Tan, T. A novel immobilization method of Saccharomyces cerevisiae to Sorghum Bagasse for Ethanol Production. *J. Biotechnol.* **2007**, *129*, 415−420.

(82) Ramakrishnan, K. R.; Padil, V. V. T.; Wacławek, S.; Černík, M.; Varma, R. S. Eco-Friendly and Economic, Adsorptive Removal of Cationic and Anionic Dyes by Bio-Based Karaya Gum—Chitosan Sponge. *Polymers* **2021**, *13*, 251.

(83) Jiang, S.; Uch, B.; Agarwal, S.; Greiner, A. Ultralight, Thermally Insulating, Compressible Polyimide Fiber Assembled Sponges. *ACS Appl. Mater. Interfaces* **2017**, *9*, 32308−32315.

(84) Guan, J.; Fujimoto, K. L.; Sacks, M. S.; Wagner, W. R. Preparation and Characterization of Highly Porous, Biodegradable Polyurethane Scaffolds for Soft tissue applications. *Biomaterials* **2005**, *26*, 3961−3971.

(85) Gonçalves, C.; Rosa Maria Rodriguez-Jasso, R. M.; Gomes, N.; JoséTeixeira, A. J. A.; Belo, I. Adaptation of Dinitrosalicylic Acid Method to Microtiter Plates. *Anal. Methods* **2010**, *2*, 2046.

(86) Bohringer, P.; Jacob, L. The Determination of Alcohol using Chromic Acid. *Zeitschr. Flussiges. Abs.* **1964**, *31*, 223.